Cerebellar-cortical function and connectivity during sensorimotor behavior in aging FMR1 gene premutation carriers

Walker S. McKinney[a], James Bartolotti[a], Pravin Khemani[b], Jun Yi Wang[c], Randi J. Hagerman[d], Matthew W. Mosconi[a,*]

[a] Life Span Institute and Kansas Center for Autism Research and Training (K-CART), Clinical Child Psychology Program, University of Kansas, 1000 Sunnyside Avenue, Lawrence, KS 66045, USA
[b] Department of Neurology, Swedish Neuroscience Institute, 550 17th Avenue, Suite 400, Seattle, WA 98122, USA
[c] Center for Mind and Brain, University of California, Davis, 267 Cousteau Place, Davis, CA 95618, USA
[d] MIND Institute and Department of Pediatrics, University of California, Davis School of Medicine, 2825 50th St., Sacramento, CA 95817, USA

ARTICLE INFO

ABSTRACT

Introduction: Premutation carriers of the *FMR1* gene are at risk of developing fragile X-associated tremor/ataxia syndrome (FXTAS), a neurodegenerative disease characterized by motor, cognitive, and psychiatric decline as well as cerebellar and cerebral white matter pathology. Several studies have documented preclinical sensorimotor issues in aging premutation carriers, but the extent to which sensorimotor brain systems are affected and may represent early indicators of atypical neurodegeneration has not been determined.
Materials and methods: Eighteen healthy controls and 16 *FMR1* premutation carriers (including five with possible, probable, or definite FXTAS) group-matched on age, sex, and handedness completed a visually guided precision gripping task with their right hand during fMRI. During the test, they used a modified pinch grip to press at 60% of their maximum force against a custom fiber-optic transducer. Participants viewed a horizontal white force bar that moved upward with increased force and downward with decreased force and a static target bar that was red during rest and turned green to cue the participant to begin pressing at the beginning of each trial. Participants were instructed to press so that the white force bar stayed as steady as possible at the level of the green target bar. Trials were 2-sec in duration and alternated with 2-sec rest periods. Five 24-sec blocks consisting of six trials were presented. Participants' reaction time, the accuracy of their force relative to the target force, and the variability of their force accuracy across trials were examined. BOLD signal change and task-based functional connectivity (FC) were examined during force vs. rest.
Results: Relative to healthy controls, premutation carriers showed increased trial-to-trial variability of force output, though this was specific to younger premutation carriers in our sample. Relative to healthy controls, premutation carriers also showed reduced extrastriate activation during force relative to rest. FC between ipsilateral cerebellar Crus I and extrastriate cortex was reduced in premutation carriers compared to controls. Reduced Crus I-extrastriate FC was related to increased force accuracy variability in premutation carriers. Increased reaction time was associated with more severe clinically rated neurological abnormalities.
Conclusions: Findings of reduced activation in extrastriate cortex and reduced Crus I-extrastriate FC implicate deficient visual feedback processing and reduced cerebellar modulation of corrective motor commands. Our results are consistent with documented cerebellar pathology and visual-spatial processing in FXTAS and presymptomatic premutation carriers, and suggest FC alterations of cerebellar-cortical networks during sensorimotor behavior may represent a "prodromal" feature associated with FXTAS degeneration.

1. Introduction

Premutation alleles of the *FMR1* gene involving 55–200 cytosine- guanine-guanine (CGG) repeats confer risk for development of fragile X-associated tremor/ataxia syndrome (FXTAS) among aging individuals (> 50 years of age). FXTAS is a neurodegenerative disorder

---

characterized by motor symptoms, including kinetic tremor and gait ataxia, radiological signs, including generalized brain atrophy, white matter pathology in the middle cerebellar peduncles (MCP) and other brain regions, as well as multiple associated clinical issues (Jacquemont et al., 2003). Molecular and demographic characteristics associated with increased FXTAS penetrance among premutation carriers have been identified, including increased age, increased CGG repeat length, increased mRNA transcript, and being male (Jacquemont et al., 2004; Leehey et al., 2008; Vittal et al., 2018; Hoem et al., 2019). The predictive value of these markers remains limited, however, and FXTAS often goes undiagnosed or diagnosed only during latter stages when symptoms become more difficult to manage (Hall et al., 2005).

FXTAS symptom presentation and timing are variable, and several studies have suggested that a "prodromal" phase, characterized by structural brain changes and subclinical social-emotional, cognitive, and motor issues may be detectable prior to clinically-observable symptoms (Wang et al., 2012; Loesch et al., 2015; Gossett et al., 2016; Wang et al., 2017; McKinney et al., 2019; Park et al., 2019). Quantitative markers of core sensorimotor and brain system differences representing prodromal FXTAS are needed to better understand disease course, identify degenerative processes during early stages, and to track and eventually mitigate disease progression, as has been done in other neurological disorders (Rowe et al., 2010; González-Garcia et al., 2011; Trujillo et al., 2015).

Multiple quantitative studies have documented sensorimotor issues in asymptomatic aging FMR1 premutation carriers, suggesting that precise sensorimotor measurements may hold promise for identifying neurodegenerative processes associated with prodromal FXTAS. Atypical postural control has been demonstrated in premutation carriers without FXTAS, including increased postural sway when presented with conflicting visual information, implicating deficits in the integration of multi-sensory feedback inputs during motor behavior (O'Keefe et al., 2015). Reduced complexity of postural sway also has been demonstrated and is associated with increased CGG repeat length in asymptomatic premutation carriers, indicating quantitative sensorimotor measurements may track with disease risk (O'Keeffe et al., 2019; Wang et al., 2019). Similarly, using tests of precision manual force, we recently documented increased motor variability in aging premutation carriers (between 44 and 77 years of age; Park et al., 2019) and reduced motor complexity associated with more severe clinical motor issues and increased CGG repeats (McKinney et al., 2019). Findings that deficits of precision manual motor control are associated with both molecular and clinical indicators of FXTAS in premutation carriers with subclinical presentations suggest that quantifiable differences in manual motor behavior may represent prodromal features of the disease. Clarifying functional brain differences associated with manual motor behavioral issues in premutation carriers may help determine new targets for identifying degeneration early in its course, similar to other diseases in which neurobiological changes can be detected prior to behavioral and clinical decline (Sommer et al., 2004; Remy et al., 2005; Unschuld et al., 2012; Dillen et al., 2017).

Manual motor control is supported by a discrete network of cortical, cerebellar, and basal ganglia circuits (Vaillancourt et al., 2003b; Prodoehl et al., 2009; Spraker et al., 2009). Cerebellar-cortical systems are selectively involved in reactively adjusting motor output in order to maintain precision in response to multi-sensory feedback error information (Stein, 1986; Wolpert et al., 1998). The MCP is the major cortical-cerebellar input pathway relaying sensory information to cerebellar targets, and hyperintensities of the MCP seen on T2-weighted MR images are a primary radiological sign of the disease (Jacquemont et al., 2003; Greco et al., 2006). MCP degeneration and more generalized cerebellar atrophy may occur before the onset of tremor, ataxia or other neurological symptoms in premutation carriers (Brunberg et al., 2002; Wang et al., 2017), and reduced MCP width is seen in both asymptomatic premutation carriers and those with FXTAS (Famula et al., 2018; Shelton et al., 2018). Further, reductions in extreme

capsule pathway connectivity (Wang et al., 2012) and superior cerebellar peduncle (SCP) tract volume are associated with increased CGG repeats and disease risk (Wang et al., 2013), suggesting that white matter pathways integrating sensorimotor brain networks are affected by FXTAS and may show degenerative changes prior to disease onset.

Task-based functional MRI studies hold particular promise for tracking disease associated neurodegeneration as they are sensitive to subtle changes in brain function and strongly related to clinical trait dimensions (Paulsen et al., 2004; Carmichael et al., 2018; Greene et al., 2018). Previous fMRI studies comparing asymptomatic premutation carriers to healthy controls have identified reduced brain activation in premutation carriers, including reduced activation in the right temporoparietal junction during a temporal working memory task (Kim et al., 2014) and reduced activation in ventral and dorsal inferior frontal cortices during a verbal working memory task (Hashimoto et al., 2011a). Reduced activation in both of these studies was shown to be associated with molecular markers known to contribute to FXTAS including increased CGG repeat length and elevated levels of FMR1 mRNA, highlighting the utility of fMRI studies in linking molecular markers to downstream brain system dysfunction. Although sensorimotor deficits are frequently observed in premutation carriers with and without FXTAS, only one known task-based functional MRI study has investigated sensorimotor control in aging premutation carriers. Brown and colleagues reported reduced activation in cerebellar lobules V-VI in asymptomatic premutation carriers during visually-guided sequential finger tapping (Brown et al., 2018). These findings suggest cerebellar dysfunction during manual motor behavior may represent a quantifiable trait dimension associated with atypical aging in premutation carriers and putative FXTAS risk. It remains unclear whether these findings reflect intrinsic defects of cerebellar function or atypical cerebellar-cortical functional connectivity as implicated by deterioration of cortical-cerebellar tracts, including the MCP and SCP, and findings of generalized white matter pathology in aging premutation carriers (Brunberg et al., 2002; Ariza et al., 2016; Sellier et al., 2017; Famula et al., 2018). Analyses of the relationships between cortical-cerebellar connectivity and precision manual motor control in aging premutation carriers are needed to clarify the functional anatomy of manual motor behavioral differences in premutation carriers and determine functional brain markers associated with the FXTAS prodrome.

In the present fMRI study, we examined cerebellar-cortical function and connectivity in aging FMR1 gene premutation carriers performing a test of visually guided precision grip force. Consistent with our prior studies (McKinney et al., 2019; Park et al., 2019), we expected FMR1 premutation carriers to show reduced force accuracy and greater force variability across trials relative to controls. We also hypothesized atypical sensory cortical and cerebellar activation and reduced cerebellar-cortical functional connectivity in premutation carriers. Sensorimotor behavior, cerebellar-cortical function, and cerebellar-cortical connectivity were analyzed in relation to CGG repeat length and clinical measures of neuromotor behavior to determine the extent to which these quantitative markers may covary with disease risk or progression.

2. Materials and methods

2.1. Participants

Sixteen FMR1 premutation carriers and 18 healthy controls completed a visually-guided precision gripping task with their right hand during fMRI. Premutation carriers and controls did not differ on age (FMR1: Median = 57 years, IQR = 48–64; Controls: Median = 55 years, IQR = 46.5–64.5; $t(32) = 0.16$, $p = .877$), sex ratio (FMR1: 25% male (N = 4); Controls: 44% male (N = 8); $\chi^2 = 1.40$, $p = .236$), handedness (FMR1: 94% right-handed (N = 15); Controls: 83% right-handed (N = 15); $\chi^2 = 0.89$, $p = .347$), full-scale IQ (FMR1: Median = 100, IQR = 94–106; Controls: Median = 106, IQR = 98.5–119.5; $t(31) = 1.99$, $p = .056$), or right hand grip strength (i.e.,

maximum voluntary contraction, or MVC; *FMR1*: Median = 39 N, IQR = 31–54; Controls: Median = 44 N, IQR = 34–54 ; $t(32) = 0.12$; $p = .904$). Based on diagnostic standards, (Jacquemont et al., 2003), one of 12 premutation carriers who completed a clinical and MRI evaluation showed signs of "possible" FXTAS, one of 12 met criteria for "probable" FXTAS, two of 12 met criteria for "definite" FXTAS, and eight of 12 showed no or insufficient clinical or radiological signs to meet diagnostic criteria for FXTAS. Of the four premutation carriers who completed only the MRI and not the clinical evaluation, two showed minor radiological signs and two showed no radiological signs of FXTAS. In total, one of 16 premutation carriers showed signs of "possible" FXTAS, two of 16 met criteria for "probable" FXTAS, two of 16 met criteria for "definite" FXTAS, eight of 16 showed limited clinical or radiological signs and did not meet FXTAS diagnostic criteria, and three of 16 were inconclusive because they showed no radiological signs specific to FXTAS but failed to complete a clinical evaluation. Clinical characteristics for all individual premutation carriers, including IQ scores, ICARS ratings, and clinical MRI findings, are provided in Table A.1.

No premutation carriers had previously received a diagnosis of any neurological disorder, including FXTAS, and no premutation carrier *self-reported* motor (e.g., gait ataxia, intention tremor) or memory issues during a clinical interview with one of the research team members (MWM). Controls were excluded for current or past neurodegenerative, neurological, or major psychiatric disorders. Controls also were excluded for a family history of fragile X syndrome or intellectual/developmental disabilities in first- or second-degree relatives. Participants from either group were excluded if they reported any known neurological or musculoskeletal disorder associated with atypical sensorimotor functioning or a history of medications known to affect sensorimotor functioning, including antipsychotics, stimulants, or benzodiazepines (Reilly et al., 2008).

FMR1 premutation carriers and healthy controls were identified using convenience sampling. *FMR1* premutation carriers geographically close enough to participate were identified through local fragile X clinics and postings on local and national fragile X association listservs. Control participants were recruited through community advertisements. All study participants provided informed consent, and all study procedures were approved by the local Institutional Review Board and were carried out in accordance with the Declaration of Helsinki.

2.2. Procedures

Cognitive functioning was assessed using the abbreviated battery of the Stanford-Binet Intelligence Scales, Fifth Edition (SB-5) including nonverbal fluid reasoning and verbal knowledge sub-sections (Roid, 2003). One participant did not complete the SB-5 because they were not fluent in English.

Thirteen premutation carriers provided blood samples to confirm *FMR1* premutation status. Premutation carriers who did not complete a blood draw provided documentation of prior genetic testing to confirm premutation carrier status. *FMR1* CGG repeat count was quantified using molecular testing conducted at Dr. Elizabeth Berry-Kravis' Molecular Diagnostic Laboratory at Rush University. Genomic DNA was isolated from peripheral blood leukocyte samples. The *FMR1* polymerase chain reaction (PCR) test with quantification of allele-specific CGG repeat count was performed using commercially available kits (Asuragen, Inc., Austin, TX). For female participants, CGG repeat analyses reflect the longest CGG repeat of the two alleles.

Twelve premutation carriers completed a clinical exam by a neurologist with expertise in movement disorders (PK). The clinical exam included administration of the International Cooperative Ataxia Rating Scale (Trouillas et al., 1997). The ICARS is comprised of 19 sections examining postural and gait disturbances, ataxia, dysarthria and oculomotor behavior. Higher scores indicate more severe neuromotor

issues. The ICARS has been validated previously for diagnosis of ataxia in patients with focal cerebellar lesions (Schoch et al., 2007), hereditary spinocerebellar and Friedrich's ataxia (Schmitz-Hubsch et al., 2006). Four premutation carriers did not complete the clinical evaluation due to scheduling difficulties. T2-weighted MR images were acquired for all 16 premutation carriers to assess radiological signs of FXTAS (PK).

2.3. Force testing

Before completing fMRI testing, each participant's right hand MVC (calculated in Newtons, or N) was estimated using the average of the maximum force output during three trials in which they pressed as hard as they could for three seconds.

During the fMRI test, participants used a modified pinch grip to press at 60% of their MVC against a custom fiber-optic transducer with 0.025 N resolution (Fig. A.1; Neuroimaging Solutions, Gainesville, FL). They viewed a horizontal white force bar that moved upward with increased force and downward with decreased force and a static target bar that was red during rest and turned green to cue the participant to begin pressing at the beginning of each trial (Fig. A.1). Participants received two instructions: (1) press the transducer as quickly as possible when the red target bar turns green, and (2) keep pressing so that the force bar stays as steady as possible at the level of the green target bar. Stimuli were presented on an EPSON PowerLite 7300 projector with a resolution of 1024 × 768 at a visual angle of 0.623°/N.

During the precision gripping task, five 24-sec blocks consisting of six trials were presented (30 trials in total). Trials were 2-sec in duration and alternated with 2-sec rest periods. Runs began with a 24-sec rest block in which participants viewed the two horizontal bars, but the bars did not move and participants were instructed not to press. Force and rest blocks then were alternated for the remainder of the run (total duration: 4:24).

2.4. Force data processing

Procedures for processing and analyzing force data were similar to those previously reported (McKinney et al., 2019). Force data were digitized at 125 Hz by an si425 Fiber Optic Interrogator (Micron Optics, Atlanta, GA) and converted to Newtons within MATLAB (National Instruments, Austin, TX). Force data were low-pass filtered with a double-pass 4th-order Butterworth filter at a 15 Hz cutoff, and analyzed using a custom algorithm previously developed by our lab and implemented in MATLAB (Wang et al., 2015). To examine force accuracy, we determined the mean sustained force for each trial and divided by the target force. Mean sustained force was examined excluding the initial phase in which individuals increased their force level, and the relaxation phase in which individuals released their force following the stop cue. We also examined the standard deviation of force accuracy across trials (force accuracy variability) and reaction time (RT). RT was calculated as the difference between the onset of gripping (when the rate of force increase first exceeded 5% of the peak rate of force increase and remained above this level for at least 100 ms) and the appearance of the start cue. Trials were excluded for off-task behavior (e.g., failure to grip after the appearance of the start cue). Premutation carriers and healthy controls did not differ in the number of valid trials (out of 30 possible trials) that were included in final analyses (*FMR1*: mean = 29.6 trials, SD = 1.5 trials; Controls: mean = 28.8 trials, SD = 2.2 trials; $t(32) = -1.22$, $p = .233$).

2.5. fMRI data acquisition

Magnetic resonance images were collected using a 3.0 T Phillips Achieva scanner with a 32-channel head coil. Anatomical images were obtained using a high-resolution T1-weighted MPRAGE sequence (TR = 8.1 ms; TE = 3.73 ms; flip angle = 12°; FOV = 256 × 204 mm^2; 160 slices; voxel size = 1 mm^3). fMRI data was acquired

using a T2*-weighted single shot, gradient-echo echo-planar pulse sequence: TR = 2000 ms; TE = 30 ms; flip angle = 60°; FOV = 220 mm^2; matrix = 64 × 64; 36 slices; voxel size = 3 × 3 × 4 mm^3. The following T2-weighted sequences was used to evaluate radiological signs of FXTAS: TR = 6350 ms; TE = 100 ms; flip angle = 120°; FOV = 256 × 256 mm^2; 78 slices; voxel size = 1 × 1 × 2 mm^3.

2.6. fMRI processing

All imaging data was processed using the Analysis of Functional Neuroimages (AFNI; https://afni.nimh.nih.gov/) software suite. Anatomical images were first uniformized, skull-stripped, and non-linearly warped to MNI standard space (MNI152) using the *@SSwarper* program. The first five volumes of each functional run were discarded to allow for magnetization equilibration. Slice-timing correction was applied using standard AFNI procedures, and consecutive volumes with > 0.5 mm of movement were discarded. All participants had < 13% of their volumes discarded due to motion, and premutation carriers and healthy controls did not differ in the percentage of TRs censored (*FMR1*: mean = 2.2%, SD = 3.9%; Controls: mean = 1.0%, SD = 3.9%; $t(32) = -1.20, p = .238$), average motion per TR (*FMR1*: mean = 0.12 mm, SD = 0.07 mm; Controls: mean = 0.12 mm, SD = 0.05 mm; $t(32) = -0.03, p = .976$), or maximum motion displacement (*FMR1*: mean = 1.46 mm, SD = 0.64 mm; Controls: mean = 1.59 mm, SD = 0.89 mm; $t(32) = 0.47, p = .644$). Remaining volumes were aligned to the nonlinearly warped, skull-stripped anatomical image using the minimum outlier volume (i.e., volume with the least movement) as a reference. Volumes were spatially smoothed to a full-width half-maximum of 5 mm and scaled to the mean voxel time-series values of 100. Regression analyses (*3dDeconvolve* and *3dREML*) for each subject used a standard block function while regressing out six motion parameters and their first derivative (x, y, z, pitch, roll, yaw). Regression BOLD signal outcomes represent percent signal change of the relevant contrast (β) and associated t-statistics.

2.7. Behavioral analysis

Linear regression analyses were conducted to compare *FMR1* premutation carriers and controls on force outcomes (i.e., RT, force accuracy, and force accuracy variability). Models included terms for group and age as well as a group × age interaction term. Age was transformed to z-scores using the grand mean for all models, and group was dummy coded with healthy controls serving as the baseline reference. Two non-normally distributed behavioral outcomes, MVC and RT, were natural log-transformed. All regression analyses were conducted using the *stats* package within R (Version 3.6.0), and effect size estimates were obtained using the *sjstats* package (Lüdecke, 2019).

2.8. Imaging analysis

A context-dependent correlation analysis (psychophysiological interaction, or PPI; Friston et al., 1997; McLaren et al., 2012) was used to compare changes in whole brain-cerebellar connectivity between groups as a function of task. Separate PPI analyses were conducted for six cerebellar seed ROIs selected based on results of prior fMRI studies of similar precision gripping tests (Vaillancourt et al., 2006; Neely et al., 2013): left and right Crus I, Crus II, and lobules V + VI. Cerebellar seeds were defined using the SUIT cerebellar atlas (Diedrichsen, 2006). Individuals' preprocessed images were analyzed using a GLM containing predictors for the Force and Rest blocks (modelled using a canonical HRF), the seed timeseries, Force × seed and Rest × seed PPI regressors, 12 motion regressors (six rotations/translations and their first derivatives), and a second-order orthogonal polynomial. PPI regressors were calculated as the interaction between the estimated neural signal from the seed region (by deconvolving the HRF) and the

Force task or Rest timeseries, which was then reconvolved with the HRF. The resulting contrast images were entered into a second-level group analysis with participant as a random effect to compare the beta weights of the two PPI regressors. Individual effect size estimates from each cluster were obtained using a leave-one-subject-out approach to preserve independence of ROI localization and estimation (Esterman et al., 2010). Specifically, for each individual, a GLM excluding that participant (using the same thresholds as the whole-group analysis) was used to localize an ROI from which that individual's mean values were extracted.

The AFNI programs *3dttest++* and *3dMEMA* were used to create separate group statistics maps and a group contrast statistics map. In light of recent concerns regarding false-positive rates in fMRI research (Eklund et al., 2016), best-practice recommendations from AFNI (Cox et al., 2017) were applied using the auto-correlation function (ACF) function within the *3dClustSim* program to correct for multiple comparisons and false positive clusters. In short, simulated noise-only volumes using ACF blur values were created, thresholded, and clustered, providing recommended cluster-size thresholds (denoted as α) to use for given voxel-wise thresholds (denoted as p). All fMRI analyses used a second nearest-neighbor (NN2) and bi-sided thresholding method. Using these methods, we present results for a family-wise error rate of $p < .01$ and cluster-size threshold of $\alpha < 0.05$ (> 49 voxels for activation differences; > 81 voxels for PPI analyses), as well as family-wise error rate of $p < .005$ and cluster-size threshold of $\alpha < 0.05$ (> 32 voxels for activation differences or > 44 for PPI analyses). After the identification of activation and connectivity clusters, linear regression models including diagnostic group, age, and a group × age interaction term as predictors were used to assess whether age-related differences in brain activation or connectivity differed between groups.

2.9. Brain-behavior analyses

To determine the relationship between age, force-related activation, force-related connectivity, and force behavior, separate linear regression analyses were conducted for RT, force accuracy, and force accuracy variability. For each model, diagnostic group was included as a predictor and brain activations that were different between premutation carriers and controls were included as predictors along with the group × brain region, age × brain region, and group × brain region × age interaction terms. Separate models were constructed for cerebellar-cortical networks identified in group PPI comparisons. A Holmes sequential Bonferroni procedure was used to calculate stepwise adjustments to the target alpha level (0.05) to control for Type I error. Due to the small number of males in our premutation carrier sample (N = 4), we did not examine sex differences or interactions. Participant sex is indicated in figures to provide case-level information.

We also assessed the relationship between force behavior, brain activation and connectivity, and CGG repeat length as well as clinical ratings of neurological abnormalities (ICARS total score). Due to the non-normal distribution of CGG repeat length and ICARS scores, the relationships between these variables, force data, BOLD signal change, and PPI outcomes were examined using Spearman's rank-order correlations. Correlational results with $p < .05$ are interpreted as significant. Correlational analyses were conducted using IBM SPSS Statistics 25.

3. Results

3.1. Precision force control in FMR1 premutation carriers and controls

Premutation carriers and healthy controls showed similar MVCs (Table A.2; β = −0.025, SE = 0.128, $p = .845$, η^2 = 0.001). Age was associated with MVC in healthy controls (β = −0.179, SE = 0.086, $p = .045$, η^2 = 0.003), though the relationship between age and MVC was different between groups (group × age: β = 0.368, SE = 0.132,

$p = .009$, $\eta^2 = 0.206$). For healthy controls, increased age was associated with lower MVCs, whereas increased age was associated with *higher* MVCs for premutation carriers.

Premutation carriers and healthy controls showed similar RTs (Table A.2; $\beta = 0.046$, SE $= 0.077$, $p = .555$, $\eta^2 = 0.011$). Age was not significantly related to RT in healthy controls ($\beta = 0.036$, SE $= 0.051$, $p = .495$, $\eta^2 = 0.005$), and the relationship between age and RT was similar across groups (group $\times$ age: $\beta = -0.048$, SE $= 0.079$, $p = .546$, $\eta^2 = 0.012$).

Visual and statistical inspection of the distribution of force accuracy values identified one significant outlier (> 4 standard deviations below the grand mean; Cook's distance $D = 0.73$) which was excluded from subsequent force accuracy analyses. Premutation carriers and healthy controls showed similar levels of force accuracy (Table A.2; $\beta = -0.004$, SE $= 0.008$, $p = .586$, $\eta^2 = 0.012$). Age was not significantly related to levels of force accuracy in healthy controls ($\beta = 0.003$, SE $= 0.005$, $p = .549$, $\eta^2 = 0.013$), and the relationship between age and force accuracy was similar across groups (group $\times$ age: $\beta = -0.014$, SE $= 0.008$, $p = .091$, $\eta^2 = 0.093$).

Overall, premutation carriers and healthy controls showed similar levels of force accuracy variability (Table A.2; $\beta = 0.009$, SE $= 0.007$, $p = .171$, $\eta^2 = 0.048$). Age was associated with force accuracy variability in healthy controls ($\beta = 0.011$, SE $= 0.004$, $p = .021$, $\eta^2 = 0.010$), though the relationship between force accuracy variability and age varied as a function of group (Fig. A.2; group $\times$ age: $\beta = -0.021$, SE $= 0.007$, $p = .005$, $\eta^2 = 0.217$). Increased age was associated with *reduced* force accuracy variability in premutation carriers and *increased* force accuracy variability in healthy controls. On average, premutation carriers under 60 years of age showed *greater* variability relative to healthy controls under 60 years of age, whereas older premutation carriers showed *less* variability than older controls.

3.2. Brain activation during force in FMR1 premutation carriers and controls

Relative to healthy controls, premutation carriers showed reduced force-dependent activation in extrastriate cortex extending from cuneus to lingual gyrus (Fig. A.3; MNI [1, -86, 7]; $k = 54$ voxels; $\beta = 0.909$). Healthy controls demonstrated greater extrastriate BOLD activation during force relative to rest ($\beta = 0.643$, $p < .01$), whereas premutation carriers showed similar activation across force and rest ($\beta = -0.266$, $p > .25$). When using a more stringent voxel-wise threshold ($p < .005$), this cluster was reduced to 31 voxels and significant only at a cluster-size threshold of $\alpha < 0.06$. Differences between groups in extrastriate activation varied as a function of age (group $\times$ age interaction: $\beta = 0.402$, SE $= 0.140$, $p = .008$, $\eta^2 = 0.142$). Increased age was associated with *reduced* extrastriate activation in controls, but *increased* extrastriate activation in premutation carriers (Fig. A.4).

3.3. Cerebellar-cortical connectivity in FMR1 premutation carriers and controls

Force-dependent changes in functional connectivity between right Crus I and extrastriate cortex (MNI [-4, 56, -2]; $k = 58$ voxels; $p < .005$, $\alpha < 0.03$) differed between groups (Fig. A.5); healthy controls showed increased Crus I-extrastriate connectivity during force compared to rest, while premutation carriers showed a decrease in Crus I-extrastriate connectivity during force compared to rest. When using a more relaxed voxel-level threshold ($p < .01$), the cluster increased in size to 75 voxels but failed to survive cluster-size thresholding ($\alpha < 0.06$). Age was not associated with Crus I-extrastriate connectivity during force ($\beta = 0.489$, SE $= 0.656$, $p = .462$, $\eta^2 = 0.018$) or rest ($\beta = 0.418$, SE $= 0.637$, $p = .517$, $\eta^2 = 0.014$). Within-group comparisons of task-dependent right Crus I connectivity are presented for controls and premutation carriers in Supplementary Fig. B.1. No other cerebellar-cortical connectivity differences were seen in comparisons of premutation carriers and healthy controls.

3.4. Cerebellar-cortical connectivity and force control

The relationships between force accuracy variability and right Crus I-extrastriate connectivity during both rest and force was different between premutation carriers and healthy controls (group $\times$ rest: $\beta = -0.013$, SE $= 0.004$, $p = .001$, $\eta^2 = 0.252$; group $\times$ force: $\beta = -0.012$, SE $= 0.004$, $p = .002$, $\eta^2 = 0.224$); increased connectivity during both rest and force was related to reduced force accuracy variability in premutation carriers but not in healthy controls (Table A.3; Fig. A.6). No other significant relationships between age, force behavior, and brain activation or connectivity were identified.

3.5. Relationships with CGG repeat length and clinical outcomes

Correlations between force outcomes, brain activation, brain connectivity, CGG repeat length and clinically rated neurological abnormalities are presented in Table A.4. Greater RTs were associated with more severe clinically rated neurological abnormalities ($\rho = 0.657$, $p = .020$). Greater force accuracy variability ($\rho = 0.366$, $p = .219$) and reduced Crus I – extrastriate connectivity during force ($\rho = -0.308$, $p = .306$) each were modestly associated with greater CGG repeat length in premutation carriers, though these relationships were not significant. No other force or brain function outcomes were associated with neurological abnormalities. Neither neurological abnormalities nor brain outcomes were associated with age.

4. Discussion

Conducting the first known task-based functional MRI study of cerebellar-cortical connectivity in aging *FMR1* premutation carriers, we document four key findings. First, premutation carriers showed increased force accuracy variability relative to controls, though this difference was specific to younger premutation carriers in our sample. In the context of a cross-sectional sample, these results suggest that aging *FMR1* premutation carriers who have remained largely asymptomatic at > 60 years of age may be less susceptible to precision motor deficiencies. Second, we document reduced extrastriate activation in aging premutation carriers relative to healthy controls during precision manual motor control indicating atypical sensorimotor behavior in premutation carriers may reflect abnormal processing of visual feedback. Consistent with our behavioral results, we also found that reductions in extrastriate activation among premutation carriers were age-dependent and may represent a key predictor of FXTAS vulnerability. Third, premutation carriers demonstrated reduced cerebellar Crus I-extrastriate functional connectivity implicating deficiencies within cortical-cerebellar networks involved in dynamically adjusting motor behavior in response to visual feedback information. Our results showing that reduced Crus I-extrastriate connectivity is related to greater force accuracy variability in premutation carriers indicates that these neural system differences are directly linked with reduced consistency of manual motor behavior. Last, slower RTs in premutation carriers were related to clinical ratings of neuromotor issues indicating that reduced capacity to rapidly execute precision manual motor actions may represent an objective and quantitative marker of clinical neurological abnormalities indicative of FXTAS.

4.1. Precision motor behavior in aging FMR1 premutation carriers

We document that aging premutation carriers show increased precision force variability relative to controls, though only during the younger ages studied here, implicating deficient sensory feedback processing of error information and alterations of motor control processes involved in dynamically adjusting output in response to error

information. These results are consistent with our prior findings of increased force variability during sustained motor action in premutation carriers (Park et al., 2019). Our finding that elevated force variability is specific to younger premutation carriers reflects an age-associated improvement in motor control (i.e., lower force accuracy variability) in premutation carriers that contrasts age-associated declines seen in our control sample and documented previously in healthy aging (Laidlaw et al., 2000; Vaillancourt et al., 2003a; Vaillancourt and Newell, 2003). In the context of our cross-sectional data, it is likely that these results highlight important differences between relatively younger and older asymptomatic premutation carriers in susceptibility to FXTAS degeneration. While FXTAS penetrance increases with age in premutation carriers, it is possible that the older premutation carriers in our sample possess background and behavioral characteristics that are protective against FXTAS as has been suggested previously (Steyaert et al., 1994; Goodrich-Hunsaker et al., 2011; McKinney et al., 2019). This is consistent with survival biases frequently observed in cross-sectional studies, in which disease-related mortality leads to the recruitment of a preponderance of individuals who are at risk for a disease but who are at lower risk for disease-related mortality (Anderson et al., 2011). The high proportion of female premutation carriers in our sample also may contribute to these findings as females are less susceptible to FXTAS (Rodriguez-Revenga et al., 2009) and demonstrate reduced clinical symptom severity (Berry-Kravis et al., 2003). Longitudinal studies of sensorimotor control in male and female premutation carriers are needed to characterize sex-specific aging profiles and determine factors that may protect against FXTAS risk and degeneration.

4.2. Cerebellar-cortical functions during precision motor behavior

We document reduced extrastriate activation in aging premutation carriers relative to controls during sensorimotor behavior implicating reduced modulatory output of extrastriate cortex or reduced translation of initial visual processing from primary visual cortex (striate cortex, or V1). During goal-directed behavior, extrastriate cortical areas modulate initial visual input to facilitate attentional selection of visual stimuli by amplifying and diminishing activity in striate cortex. Reduced activation of extrastriate cortex in premutation carriers may reflect difficulties attending to and processing basic visual input during rapid motor action. These findings extend the one known prior fMRI study of motor behavior in premutation carriers to indicate that decreased modulation of precision motor behavior in premutation carriers is associated with reduced processing of sensory feedback information (Brown et al., 2018). We also found that extrastriate functional differences in premutation carriers were age-dependent; increased age was associated with *increased* extrastriate activation in premutation carriers, but *reduced* extrastriate activation in controls. These findings suggest extrastriate hypoactivation during sensorimotor behavior may be an important marker of FXTAS vulnerability among aging premutation carriers whereas older premutation carriers who have not shown any signs of degeneration may represent a more resilient subgroup characterized by more "normative" patterns of aging. As the majority of our sample was female, these findings also may indicate that older female premutation carriers in our sample, who are less likely to develop FXTAS given that they are female and beyond the median age of FXTAS onset (i.e., ~60 years), may be resistant to the severe degeneration seen in FXTAS. Longitudinal studies are needed to characterize aging processes of sensorimotor brain network functions in male and female premutation carriers.

Reduced extrastriate activation in premutation carriers may reflect structural degeneration of posterior medial cortical circuits including extrastriate and white matter input pathways to extrastriate cortex, such as optic radiations or posterior splenium. Initial visual input is transmitted to visual cortices through projections from lateral geniculate nucleus via the geniculo-striatal pathway (Rathbun and Usrey, 2009). Impaired visual motion processing has been documented in premutation carriers (Kéri and Benedek, 2009; 2012), suggesting pathology within geniculo-striatal magnocellular pathways may contribute to reductions in downstream

extrastriate activation. Reduced extrastriate activation in our sample also is consistent with findings of degeneration of the splenium of the corpus callosum in aging premutation carriers. During visual processing, interhemispheric striate and extrastriate visual information converge within the splenium (Dougherty et al., 2005). Hyperintensities within the splenium have been observed in individuals with FXTAS, especially females (Adams et al., 2007; Apartis et al., 2012). Our finding of reduced extrastriate activation in our largely female sample of premutation carriers may reflect alterations in posterior splenium projections that interfere with sensorimotor behavior. Our study did not include a large enough sample of male premutation carriers to systematically assess sex differences in brain activation, but larger studies comparing male and female premutation carrier brain activation during sensorimotor behavior and visual processing are warranted.

We also provide novel evidence that precision sensorimotor differences in aging premutation carriers are associated with reduced cerebellar Crus I-extrastriate (BA 18/19) connectivity. During sensorimotor action, visual input is processed in V1 before extrastriate cortical areas encode stimulus features including shape, color, form and motion information (Hampson et al., 2004; Born and Bradley, 2005; Arcaro and Kastner, 2015). These circuits have reciprocal connections with posterior parietal cortex (PPC) and inferior temporal association areas (Colby et al., 1988; Baizer et al., 1991) where higher-level information, including spatial and featural information, respectively, is processed and relayed to cerebellum. The medial extrastriate target we identified in our group findings also has been shown to integrate multimodal information, including different sensory inputs that may be relayed to cerebellum to guide refinements of ongoing motor behavior (Glickstein et al., 1985; Macaluso et al., 2002). Differences between sensory feedback information and the efferent copy transmitted from M1 to cerebellum are computed within cerebellar cortex, and the refined motor command is translated to PPC and M1 to modify motor output and improve the accuracy of subsequent action (Stein and Glickstein, 1992; Glickstein, 2000; Vaillancourt et al., 2003b). Our findings of reduced extrastriate activation and Crus I-extrastriate connectivity in premutation carriers indicates deficient processing of multi-sensory feedback and communication between sensory processing circuits and cerebellum. Our specific result that, relative to healthy controls, premutation carriers demonstrated reductions in Crus I-extrastriate connectivity during force relative to rest implicates a reduced ability to integrate multiple cortical-cerebellar pathways during sensorimotor behavior. Importantly, reduced Crus I-extrastriate connectivity was strongly related to reduced force accuracy variability in premutation carriers whereas extrastriate activation was not associated with sensorimotor behavior, suggesting cerebellar-cortical connectivity may better capture the neurophysiological substrates of motor decline in premutation carriers at risk for FXTAS relative to intrinsic activation of local circuits. Additionally, when examined separately, neither premutation carriers nor healthy controls demonstrated significant changes in connectivity between force and rest. It is possible that the relative decrease in Crus I-extrastriate connectivity during force in premutation carriers compared to healthy controls is driven by a true reduction in connectivity upon the application of force in premutation carriers that we were unable to detect due to limited power in identifying relatively smaller effect sizes (e.g., premutation carrier within-group percent signal change of −0.549). A true decrease in connectivity upon the application of force in premutation carriers could reflect cerebellar or splenium degeneration in premutation carriers that disrupts the integration of cerebellar-cortical processes during sensorimotor control.

Our findings of reduced Crus I-extrastriate connectivity are consistent with prior structural MRI and histopathological studies showing white matter degeneration in premutation carriers with and without FXTAS (Greco et al., 2006; Hashimoto et al., 2011b; Famula et al., 2018). Cortical innervation of cerebellar cortex primarily is translated via pontine nuclei and MCP. Our findings suggest that frequently documented MCP degeneration in FXTAS and asymptomatic premutation carriers may disrupt cortical-cerebellar input processes, including sensory feedback modulation of motor behavior (Cohen et al., 2006; Wang et al., 2017; Famula et al., 2018; Shelton et al., 2018). Input to

cerebellar cortex through MCP pathways occurs through white matter fiber tracts terminating on dendritic spines of Purkinje cells. Purkinje cell pathology, including reduced cell number and ubiquitin-positive intranuclear inclusions, has been documented in post-mortem brain studies of premutation carriers (Greco et al., 2006; Ariza et al., 2016). Broadly, our fMRI results suggest that quantifying functional connectivity of cortical-cerebellar pathways during motor behavior may provide objective approaches for tracking cerebellar and sensorimotor degeneration in aging premutation carriers and marking putative prodromal neurobiological processes associated with FXTAS.

4.3. Sensorimotor behavior, genetic outcomes, and neurological abnormalities

We found that the relationships between CGG repeat length and both force accuracy variability and Crus I-extrastriate functional connectivity were of medium effect size (r's > 0.3; Cohen, 1992), though neither were significant. While it is possible that these relationships were not significant due to our relatively small sample size, several other factors also should be considered. First, measures of CGG repeat length may fail to capture downstream molecular processes that are more strongly linked with sensorimotor and functional connectivity alterations. This is especially notable in a mixed-sex sample comprised of 75% females who may show variable activation ratios. Additional measurements including activation ratio, mRNA transcript, and AGG interruptions will be necessary to identify molecular mechanisms contributing to sensorimotor and neural system changes and better estimate disease risk and progression. Second, cross-sectional measures of force variability and cerebellar-cortical connectivity may be less sensitive to neurodegenerative processes associated with molecular markers and FXTAS. While the quantitative behavioral and imaging approaches described here and those documented previously (O'Keefe et al., 2016; Wang et al., 2017; Famula et al., 2018; Shelton et al., 2018) show promise for identifying prodromal markers of FXTAS, longitudinal studies tracking these outcomes over time in premutation carriers are needed to determine their prognostic value.

We replicated our prior finding of an association between increased reaction time and more severe clinically rated neurological abnormalities in aging premutation carriers, although it should be noted that the premutation carriers in the present study also participated in our prior behavioral study (McKinney et al., 2019). Deficits in the rapid execution of precision manual motor actions may reflect multiple issues including delayed information processing or action execution at peripheral or central levels (Soontarapornchai et al., 2008). This is consistent with our prior findings of reduced motor unit discharge rate (Park et al., 2019). Efficient processing of sensory information and the transmission of motor commands to initiate movement also rely on intact white matter structural networks which may be affected in premutation carriers, as indicated by prior findings of reduced structural connectivity of white matter motor fiber tracts in FXTAS patients as well as findings of associations between molecular and genetic markers and reduced structural connectivity in asymptomatic premutation carriers (Wang et al., 2013). These results may be related to the bradykinesia previously documented in FXTAS patients (Niu et al., 2014) and may represent a distinct motor marker of degeneration relative to the control of precision output. We used a fixed inter-trial rest interval during our sensorimotor task in this study suggesting that increased RTs may reflect reduced ability to anticipate the timing of patterned behavior (Johari and Behroozmand, 2017). Direct comparisons of fixed and variable inter-trial intervals during rapid motor actions will be important for characterizing predictive motor processes and their neural substrates in premutation carriers.

4.4. Limitations and future directions

Our study has several limitations that should be addressed in future work. First, longitudinal studies will aid in determining the value of cerebellar-cortical connectivity and our behavioral measurements as prodromal markers of FXTAS. It is unknown whether these neurological and biobehavioral markers are specific to premutation carriers who will develop FXTAS or are present across the majority of premutation carriers. These and previous results documenting relationships between behavioral measurements and symptom severity, however, suggest that quantifiable markers of sensorimotor precision track with clinical severity and may serve as early diagnostic markers (Kraan et al., 2014; O'Keefe et al., 2016; McKinney et al., 2019; Wang et al., 2019). Larger samples representative of the broad range of sensorimotor and neurological functioning observed in aging premutation carriers will help assess which measures are most sensitive to early decline. Second, studies comparing aging effects on sensorimotor behavior and brain function in male and female premutation carriers are needed. The majority of our premutation carrier sample was female, though few quantitative studies have assessed sensorimotor behavior in aging female premutation carriers, and no known fMRI studies have examined sensorimotor brain function in aging female premutation carriers. Our results indicate that aging female, and not just male premutation carriers show sensorimotor and cerebellar-cortical differences compared to controls. It is possible that our findings are specific to female premutation carriers, though we would expect male premutation carriers to show similar or more severe sensorimotor and cerebellar-cortical differences given that they are more likely to develop FXTAS and demonstrate sensorimotor and cerebellar degeneration (Jacquemont et al., 2004; Greco et al., 2006; Coffey et al., 2008). Prior studies showing that degeneration of the splenium is more common in female than male premutation carriers (Adams et al., 2007; Apartis et al., 2012) indicate that mechanisms of sensorimotor deterioration may vary as a function of sex. Still, our results suggest that our behavioral and brain markers may be robust to sensorimotor and functional brain differences in premutation carriers across sex. Third, integration of multiple molecular markers associated with FXTAS are needed, including mRNA transcript, RAN, and mitochondrial function (Todd et al., 2013; Sellier et al., 2017; Isabel Alvarez-Mora et al., 2020). Integration of information across molecular, brain, and behavioral levels will guide more individualized models of neurodegenerative processes associated with *FMR1* premutations, and determine prodromal characteristics associated with FXTAS.

5. Conclusions

Our study indicates that reduced cortical-cerebellar functional connectivity and sensorimotor precision are associated with aging in *FMR1* premutation carriers. Dysfunction of cortical-cerebellar pathways may represent early degenerative processes associated with prodromal FXTAS. FMRI measurements of cortical-cerebellar connectivity during precision motor behavior appear to be useful, objective outcomes for tracking distinct aging patterns in premutation carriers in order to understand degenerative processes and perhaps determine disease risk as premutation carriers age.

Appendix A

Table A.1
Demographic and clinical characteristics of *FMR1* premutation carriers.

Subject	Age	Sex	FSIQ	CGG repeat length	ICARS total score	Radiological findings	Jacquemont et al., 2003 categorization
1	48	F	100	–	–	No signs	Inconclusive
2	56	F	100	87	2	Generalized cerebral WM lesion, cerebral atrophy (type 1)	Non-FXTAS
3	62	F	115	102	3	Generalized cerebral WM lesion, cerebral atrophy (type 2)	Non-FXTAS
4	71	M	103	85	12	MCP sign, generalized cerebral WM lesion, cerebral atrophy (type 3)	Definite
5*	46	F	100	–	–	Mild cerebral WM lesion, dot-like cerebral WM hyperintensities	Probable
6	58	M	94	60	4	No signs	Non-FXTAS
7	58	M	94	63	2	No signs	Non-FXTAS
8	52	F	106	81	5	Cerebral atrophy (type 1)	Probable
9	67	F	109	62	2	Mild cerebral WM lesion, dot-like cerebral WM hyperintensities	Possible
10	48	F	106	110	5	No signs	Non-FXTAS
11	46	F	100	68	0	Mild cerebral WM lesion, dot-like cerebral WM hyperintensities	Non-FXTAS
12	64	F	94	80	1	Mild cerebral WM lesion, dot-like cerebral WM hyperintensities, cerebral atrophy (type 2)	Non-FXTAS
13	49	F	–	55	0	MCP sign	Non-FXTAS
14	44	F	100	81	–	Mild cerebellar atrophy	Inconclusive
15	57	M	61	93	8	MCP sign, cerebral atrophy (type 1), widening of 4th ventricle, cerebellar/brainstem atrophy	Definite
16	65	F	106	–	–	No signs	Inconclusive

FSIQ: full-scale IQ; CGG: cytosine-guanine-guanine; ICARS: International Cooperative Ataxia Rating Scale; WM: white matter; MCP: middle cerebellar peduncle; Jacquemont et al., 2003 criteria are as follows: "definite" – one major clinical sign plus one major radiological sign; "probable" – either one major radiological sign plus one minor clinical sign or two major clinical signs; "possible" – one major clinical sign plus one minor radiological sign; *Subject 5 did not complete a clinical evaluation but review of medical records indicated the participant demonstrated both gait ataxia and kinetic tremor (both major clinical signs of FXTAS).

Table A.2
Best fitting linear regression models for sensorimotor behavior group comparisons.

MVC	**Term**	**Estimate (SE)**	***t(30)***	**η²**
	Intercept	3.734 (0.088)	42.421*	–
	Group	−0.025 (0.128)	−0.197	0.001
	Age	−0.179 (0.086)	−2.087*	0.003
	Group × Age	0.368 (0.132)	2.795*	0.206
Reaction time	**Term**	**Estimate (SE)**	***t(30)***	**η²**
	Intercept	−0.952 (0.053)	−17.953*	–
	Group	0.046 (0.077)	0.597	0.011
	Age	0.036 (0.051)	0.691	0.005
	Group × Age	−0.048 (0.079)	−0.611	0.012
Force accuracy	**Term**	**Estimate (SE)**	***t(29)***	**η²**
	Intercept	0.992 (0.005)	186.555*	–
	Group	−0.004 (0.008)	−0.552	0.012
	Age	0.003 (0.005)	0.606	0.013
	Group × Age	−0.014 (0.008)	−1.750	0.093
Force accuracy variability	**Term**	**Estimate (SE)**	***t(30)***	**η²**
	Intercept	0.042 (0.005)	9.131*	–
	Group	0.009 (0.007)	1.402	0.048
	Age	0.011 (0.004)	2.437*	0.010
	Group × Age	−0.021 (0.007)	−2.994*	0.217

*$p < .05$; MVC: maximum voluntary contraction; MVC and RT were natural log-transformed.

Table A.3
Best fitting linear regression models for right Crus I-extrastriate connectivity and force accuracy variability relationship.

Force accuracy variability	Crus I-extrastriate connectivity during rest	Term	Estimate (SE)	*t(29)*	η²
		Intercept	0.042 (0.004)	10.195*	–
		Group	0.015 (0.006)	2.385*	0.048
		Age	0.004 (0.003)	1.238	0.012
		PPI during rest	0.004 (0.002)	0.134	0.121
		Group × PPI during rest	−0.013 (0.004)	−3.592*	0.252
	Crus I-extrastriate connectivity during force	Term	Estimate (SE)	*t(29)*	η²
		Intercept	0.047 (0.003)	15.357*	–
		Group	0.010 (0.006)	1.677	0.048
		Age	0.004 (0.003)	1.216	0.012
		PPI during force	−0.005 (0.002)	−3.077*	0.129
		Group × PPI during force	−0.012 (0.004)	−3.332*	0.224

*$p < .05$; PPI: psychophysiological interaction.

Table A.4
Clinical and demographic associations.

Variable	CGG repeat length	ICARS total score	Reaction time	Force accuracy	Force accuracy variability	PPI during force
Age[†]	−0.066	0.258	0.096	−0.113	0.095	0.027
CGG repeat length[††]	–	0.562*	0.391	0.047	0.366	−0.308
ICARS total score[††]	–	–	0.657*	−0.187	0.244	−0.194
Reaction time[†]	–	–	–	−0.310	0.350*	−0.231
Force accuracy[†]	–	–	–	–	−0.109	−0.041
Force accuracy variability[†]	–	–	–	–	–	−0.370*

CGG: cytosine-guanine-guanine; ICARS: International Cooperative Ataxia Rating Scale; PPI reflects right Crus I – extrastriate connectivity during the force condition; *$p < .05$; [†]Pearson correlations for combined healthy controls and premutation carriers; [††]Spearman rank-order correlations for premutation carriers only.

Fig. A.1. Sensorimotor test stimuli and custom fiber-optic transducer (C; Neuroimaging Solutions, Gainesville, FL). Participants pressed when the red bar (A) turned green (B) in order to move the white bar up to the target green bar. They were instructed to maintain their force level at the level of the green bar as steadily as possible.
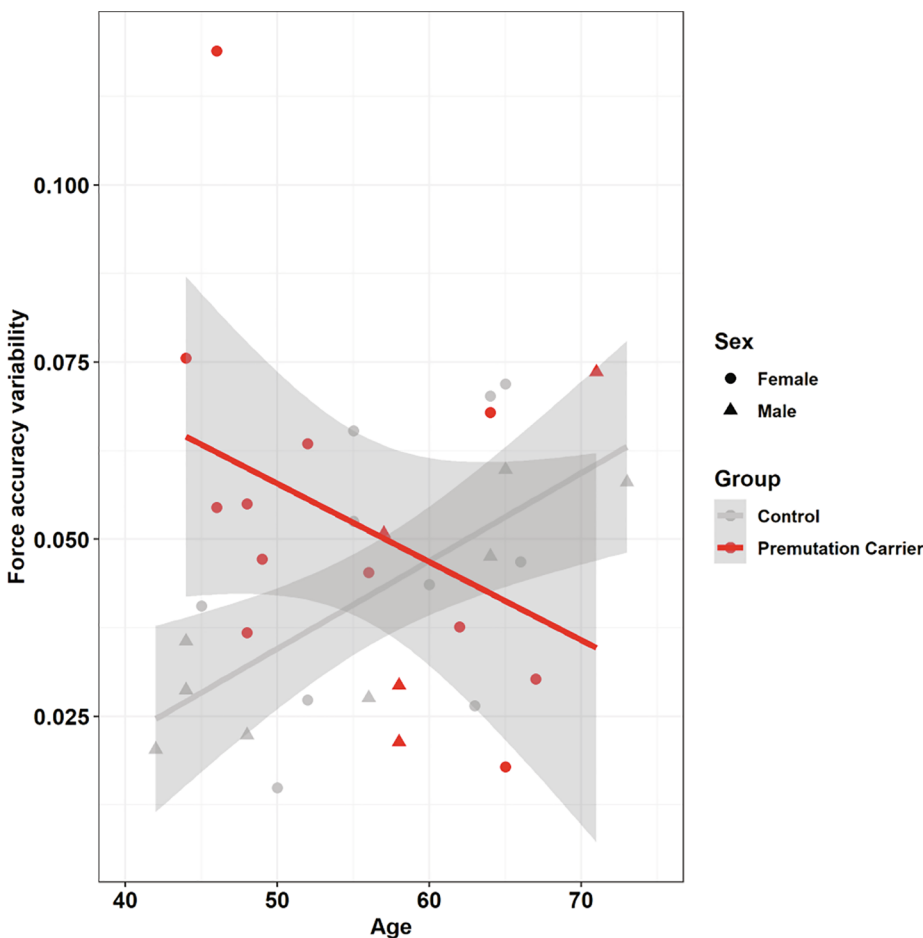

Fig. A.2. The relationship between force accuracy variability and age varied as a function of group. Post hoc analyses indicated that increased age was associated with *reduced* force accuracy variability in premutation carriers (i.e., more consistent performance) and *increased* force accuracy variability in healthy controls (i.e., less consistent performance). Shaded regions reflect the 95% confidence interval of a group-level linear fit.
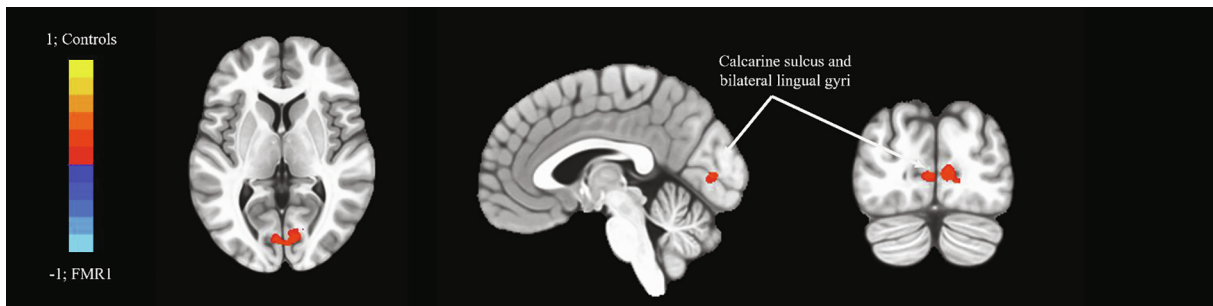
Fig. A.3. BOLD activation contrast map of force compared to rest for healthy controls vs. *FMR1* premutation carriers. Relative to *FMR1* premutation carriers, healthy controls demonstrated greater BOLD signal in extrastriate cortex during force relative to rest. MNI coordinates: [1, −86, 7]; $k = 54$ voxels; $\beta = 0.909$; $p < .01$, $\alpha < 0.05$.
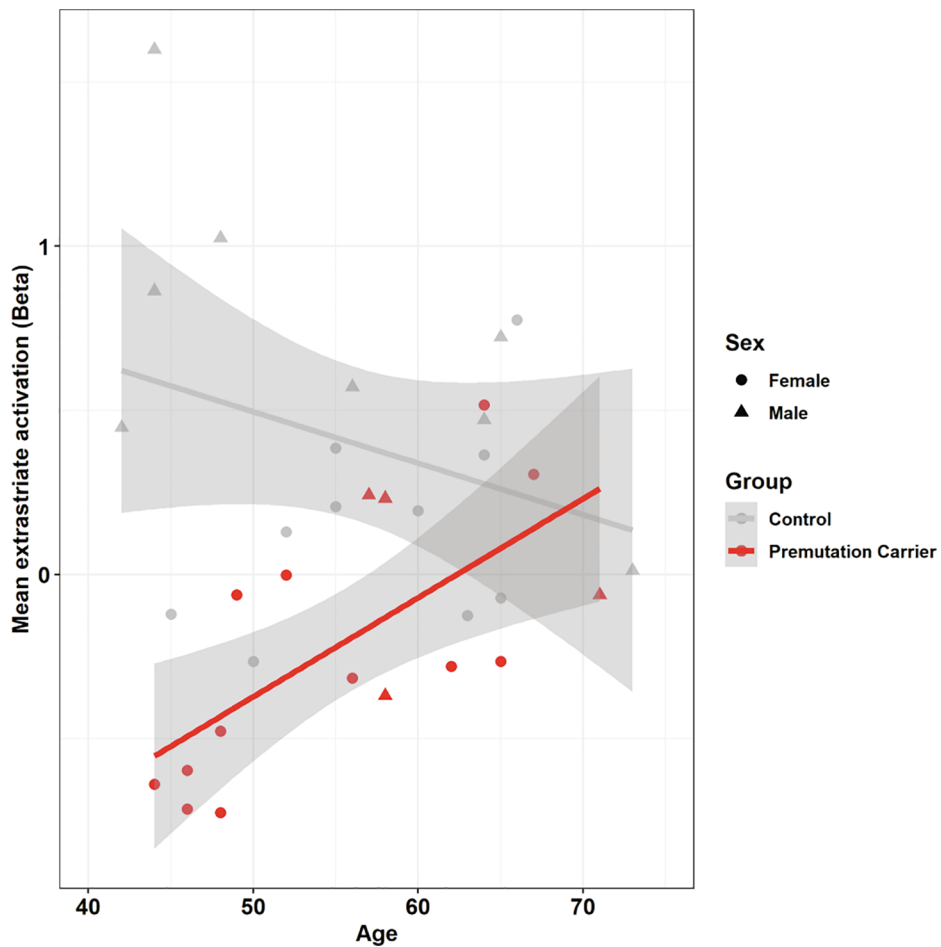

Fig. A.4. Relationship between extrastriate BOLD activation (force minus rest) and age for healthy controls vs. *FMR1* premutation carriers. Premutation carriers showed increased extrastriate activation with age, while healthy controls showed reduced extrastriate activation with age. Shaded regions reflect the 95% confidence interval of a group-level linear fit.
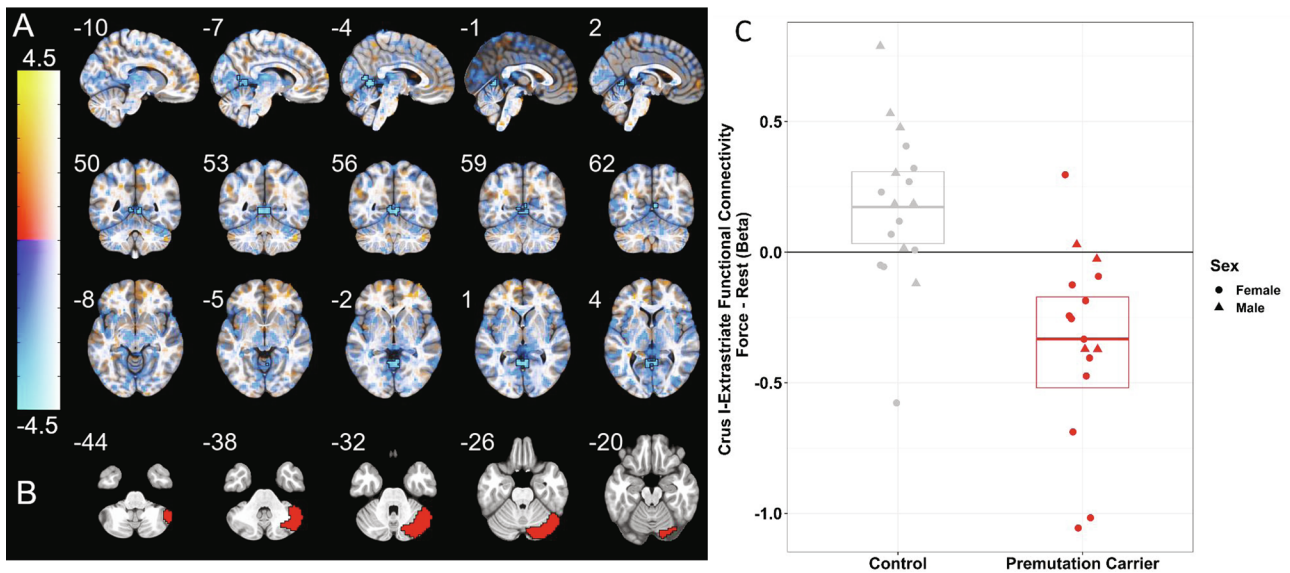
Fig. A.5. Group differences in task-dependent right Crus I connectivity. A) Connectivity between right Crus I and a cluster in extrastriate cortex increased during force relative to rest in controls, but decreased during force relative to rest in *FMR1* premutation carriers. Blue indicates a larger force – rest interaction in controls compared to premutation carriers. Orange indicates a larger force-rest change in premutation carriers. Whole-brain effects are displayed, and a significant cluster in extrastriate cortex is outlined in black (voxel $p < .005$, cluster $\alpha < 0.03$). B) Right Crus I seed region. C) Beta weights for force and rest PPI regressors were estimated using a leave-one-subject-out method. Error bars represent the mean and bootstrap estimated ± 1 standard error.
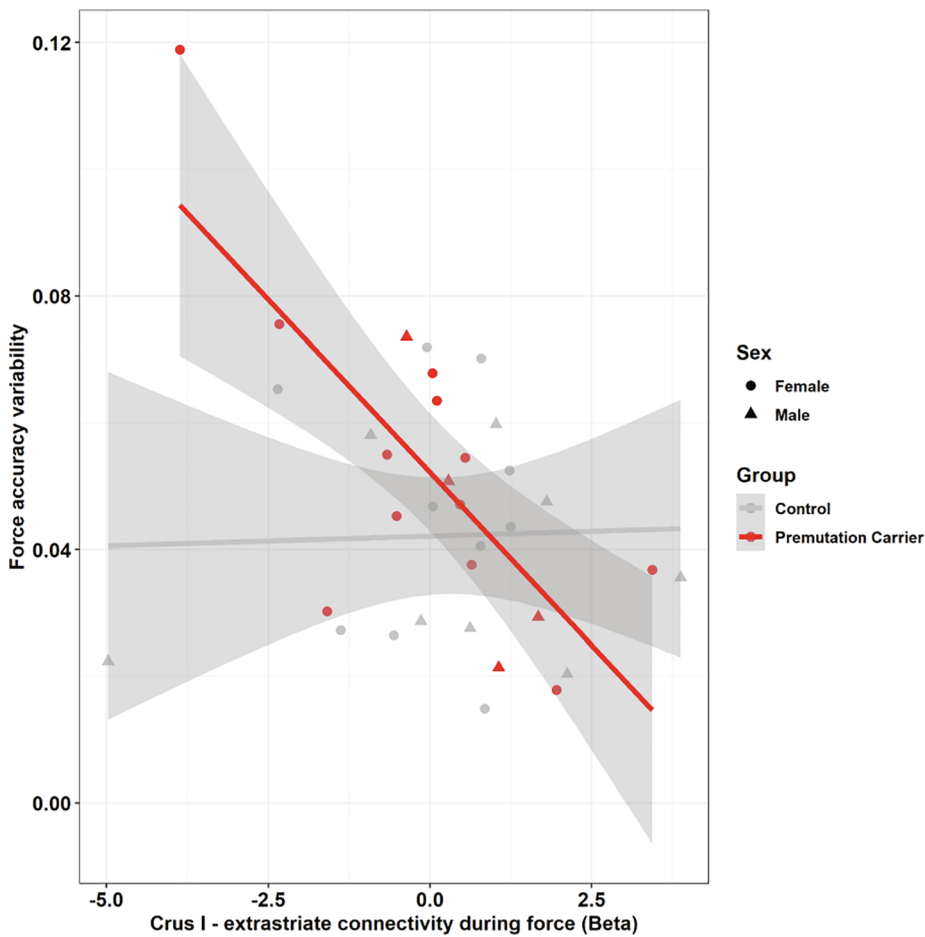

Fig. A.6. Relationship between force accuracy variability on Crus I-extrastriate functional connectivity. Greater Crus I-extrastriate functional connectivity was associated with lower force accuracy variability in premutation carriers but not in healthy controls. Shaded regions reflect the 95% confidence interval of a group-level linear fit.

Appendix B. Supplementary data

Supplementary data to this article can be found online at https://doi.org/10.1016/j.nicl.2020.102332.

References

Adams, J.S., Adams, P.E., Nguyen, D., Brunberg, J.A., Tassone, F., Zhang, W., et al., 2007. Volumetric brain changes in females with fragile X-associated tremor/ataxia syndrome (FXTAS). Neurology 69 (9), 851–859. https://doi.org/10.1212/01.wnl.0000269781.10417.7b.

Anderson, C.D., Nalls, M.A., Biffi, A., Rost, N.S., Greenberg, S.M., Singleton, A.B., et al., 2011. The effect of survival bias on case-control genetic association studies of highly lethal diseases. Circ. Cardiovasc. Genet. 4 (2), 188–196. https://doi.org/10.1161/CIRCGENETICS.110.957928.

Apartis, E., Blancher, A., Meissner, W.G., Guyant-Marechal, L., Maltete, D., De Broucker, T., et al., 2012. FXTAS: new insights and the need for revised diagnostic criteria. Neurology 79 (18), 1898–1907. https://doi.org/10.1212/WNL.0b013e318271f7ff.

Arcaro, M.J., Kastner, S., 2015. Topographic organization of areas V3 and V4 and its relation to supra-areal organization of the primate visual system. Vis. Neurosci. 32, E014. https://doi.org/10.1017/S0952523815000115.

Ariza, J., Rogers, H., Monterrubio, A., Reyes-Miranda, A., Hagerman, P.J., Martinez-Cerdeno, V., 2016. A majority of FXTAS cases present with intranuclear inclusions within Purkinje cells. Cerebellum 15 (5), 546–551. https://doi.org/10.1007/s12311-016-0776-y.

Baizer, J.S., Ungerleider, L.G., Desimone, R., 1991. Organization of visual inputs to the inferior temporal and posterior parietal cortex in macaques. J. Neurosci. 11 (1), 168–190.

Berry-Kravis, E., Lewin, F., Wuu, J., Leehey, M., Hagerman, R., Hagerman, P., et al., 2003. Tremor and ataxia in fragile X premutation carriers: blinded videotape study. Ann. Neurol. 53 (5), 616–623. https://doi.org/10.1002/ana.10522.

Born, R.T., Bradley, D.C., 2005. Structure and function of visual area MT. Annu. Rev. Neurosci. 28, 157–189. https://doi.org/10.1146/annurev.neuro.26.041002.131052.

Brown, S.S.G., Basu, S., Whalley, H.C., Kind, P.C., Stanfield, A.C., 2018. Age-related functional brain changes in FMR1 premutation carriers. Neuroimage Clin. 17, 761–767. https://doi.org/10.1016/j.nicl.2017.12.016.

Brunberg, J.A., Jacquemont, S., Hagerman, R.J., Berry-Kravis, E.M., Grigsby, J., Leehey, M.A., et al., 2002. Fragile X premutation carriers: characteristic MR imaging findings of adult male patients with progressive cerebellar and cognitive dysfunction. AJNR Am. J. Neuroradiol. 23 (10), 1757–1766.

Carmichael, O., Schwarz, A.J., Chatham, C.H., Scott, D., Turner, J.A., Upadhyay, J., et al., 2018. The role of fMRI in drug development. Drug Discov. Today 23 (2), 333–348. https://doi.org/10.1016/j.drudis.2017.11.012.

Coffey, S.M., Cook, K., Tartaglia, N., Tassone, F., Nguyen, D.V., Pan, R., et al., 2008. Expanded clinical phenotype of women with the FMR1 premutation. Am. J. Med. Genet. A 146A (8), 1009–1016. https://doi.org/10.1002/ajmg.a.32060.

Cohen, J., 1992. A power primer. Psychol. Bull. 112 (1), 155–159. https://doi.org/10.1037//0033-2909.112.1.155.

Cohen, S., Masyn, K., Adams, J., Hessl, D., Rivera, S., Tassone, F., et al., 2006. Molecular and imaging correlates of the fragile X-associated tremor/ataxia syndrome. Neurology 67 (8), 1426–1431. https://doi.org/10.1212/01.wnl.0000239837.57475.3a.

Colby, C.L., Gattass, R., Olson, C.R., Gross, C.G., 1988. Topographical organization of cortical afferents to extrastriate visual area po in the macaque – a dual tracer study. J. Comp. Neurol. 269 (3), 392–413. https://doi.org/10.1002/cne.902690307.

Cox, R.W., Chen, G., Glen, D.R., Reynolds, R.C., Taylor, P.A., 2017. FMRI clustering in AFNI: false-positive rates redux. Brain Connect. 7 (3), 152–171. https://doi.org/10.1089/brain.2016.0475.

Diedrichsen, J., 2006. A spatially unbiased atlas template of the human cerebellum. Neuroimage 33 (1), 127–138. https://doi.org/10.1016/j.neuroimage.2006.05.056.

Dillen, K.N.H., Jacobs, H.I.L., Kukolja, J., Richter, N., von Reutern, B., Onur, O.A., et al., 2017. Functional disintegration of the default mode network in prodromal alzheimer's disease. J. Alzheimers Dis. 59 (1), 169–187. https://doi.org/10.3233/JAD-161120.

Dougherty, R.F., Ben-Shachar, M., Bammer, R., Brewer, A.A., Wandell, B.A., 2005. Functional organization of human occipital-callosal fiber tracts. Proc. Natl. Acad. Sci. U.S.A 102 (20), 7350–7355. https://doi.org/10.1073/pnas.0500003102.

Eklund, A., Nichols, T.E., Knutsson, H., 2016. Cluster failure: Why fMRI inferences for spatial extent have inflated false-positive rates. Proc. Natl. Acad. Sci. U.S.A 113 (28), 7900–7905. https://doi.org/10.1073/pnas.1602413113.

Esterman, M., Tamber-Rosenau, B.J., Chiu, Y.C., Yantis, S., 2010. Avoiding non-independence in fMRI data analysis: leave one subject out. Neuroimage 50 (2), 572–576. https://doi.org/10.1016/j.neuroimage.2009.10.092.

Famula, J.L., McKenzie, F., McLennan, Y.A., Grigsby, J., Tassone, F., Hessl, D., et al., 2018. Presence of middle cerebellar peduncle sign in FMR1 premutation carriers without tremor and ataxia. Front. Neurol. 9, 695. https://doi.org/10.3389/fneur.2018.00695.

Friston, K.J., Buechel, C., Fink, G.R., Morris, J., Rolls, E., Dolan, R.J., 1997. Psychophysiological and modulatory interactions in neuroimaging. Neuroimage 6 (3), 218–229. https://doi.org/10.1006/nimg.1997.0291.

Glickstein, M., 2000. How are visual areas of the brain connected to motor areas for the sensory guidance of movement? Trends Neurosci. 23 (12), 613–617.

Glickstein, M., May 3rd, J.G., Mercier, B.E., 1985. Corticopontine projection in the

macaque: the distribution of labelled cortical cells after large injections of horse-radish peroxidase in the pontine nuclei. J. Comp. Neurol. 235 (3), 343–359. https://doi.org/10.1002/cne.902350306.

González-Garcia, N., Armony, J.L., Soto, J., Trejo, D., Alegria, M.A., Drucker-Colin, R., 2011. Effects of rTMS on Parkinson's disease: a longitudinal fMRI study. J. Neurol. 258 (7), 1268–1280. https://doi.org/10.1007/s00415-011-5923-2.

Goodrich-Hunsaker, N.J., Wong, L.M., McLennan, Y., Tassone, F., Harvey, D., Rivera, S.M., et al., 2011. Enhanced manual and oral motor reaction time in young adult female fragile X premutation carriers. J. Int. Neuropsychol. Soc. 17 (4), 746–750. https://doi.org/10.1017/S1355617711000634.

Gossett, A., Sansone, S., Schneider, A., Johnston, C., Hagerman, R., Tassone, F., et al., 2016. Psychiatric disorders among women with the fragile X premutation without children affected by fragile X syndrome. Am. J. Med. Genet. B Neuropsychiatr. Genet. 171 (8), 1139–1147. https://doi.org/10.1002/ajmg.b.32496.

Greco, C.M., Berman, R.F., Martin, R.M., Tassone, F., Schwartz, P.H., Chang, A., et al., 2006. Neuropathology of fragile X-associated tremor/ataxia syndrome (FXTAS). Brain 129 (Pt 1), 243–255. https://doi.org/10.1093/brain/awh683.

Greene, A.S., Gao, S., Scheinost, D., Constable, R.T., 2018. Task-induced brain state manipulation improves prediction of individual traits. Nat. Commun. 9 (1), 2807. https://doi.org/10.1038/s41467-018-04920-3.

Hall, D.A., Berry-Kravis, E., Jacquemont, S., Rice, C.D., Cogswell, J., Zhang, L., et al., 2005. Initial diagnoses given to persons with the fragile X associated tremor/ataxia syndrome (FXTAS). Neurology 65 (2), 299–301. https://doi.org/10.1212/01.wnl.0000168900.86323.9c.

Hampson, M., Olson, I.R., Leung, H.C., Skudlarski, P., Gore, J.C., 2004. Changes in functional connectivity of human MT/V5 with visual motion input. NeuroReport 15 (8), 1315–1319. https://doi.org/10.1097/01.wnr.0000129997.95055.15.

Hashimoto, R., Backer, K.C., Tassone, F., Hagerman, R.J., Rivera, S.M., 2011a. An fMRI study of the prefrontal activity during the performance of a working memory task in premutation carriers of the fragile X mental retardation 1 gene with and without fragile X-associated tremor/ataxia syndrome (FXTAS). J. Psychiatr. Res. 45 (1), 36–43. https://doi.org/10.1016/j.jpsychires.2010.04.030.

Hashimoto, R., Srivastava, S., Tassone, F., Hagerman, R.J., Rivera, S.M., 2011b. Diffusion tensor imaging in male premutation carriers of the fragile X mental retardation gene. Mov. Disord. 26 (7), 1329–1336. https://doi.org/10.1002/mds.23646.

Hoem, G., Bowitz Larsen, K., Overvatn, A., Brech, A., Lamark, T., Sjottem, E., et al., 2019. The FMRpolyGlycine protein mediates aggregate formation and toxicity independent of the CGG mRNA hairpin in a cellular model for FXTAS. Front. Genet. 10, 249. https://doi.org/10.3389/fgene.2019.00249.

Isabel Alvarez-Mora, M., Santos, C., Carreno-Gago, L., Madrigal, I., Isabel Tejada, M., Martinez, F., et al., 2020. Role of mitochondrial DNA variants in the development of fragile X-associated tremor/ataxia syndrome. Mitochondrion. https://doi.org/10.1016/j.mito.2020.03.004.

Jacquemont, S., Hagerman, R.J., Leehey, M., Grigsby, J., Zhang, L., Brunberg, J.A., et al., 2003. Fragile X premutation tremor/ataxia syndrome: Molecular, clinical, and neuroimaging correlates. Am. J. Hum. Genet. 72 (4), 869–878. https://doi.org/10.1086/374321.

Jacquemont, S., Hagerman, R.J., Leehey, M.A., Hall, D.A., Levine, R.A., Brunberg, J.A., et al., 2004. Penetrance of the fragile X-associated tremor/ataxia syndrome in a premutation carrier population. JAMA 291 (4), 460–469. https://doi.org/10.1001/jama.291.4.460.

Johari, K., Behroozmand, R., 2017. Temporal predictive mechanisms modulate motor reaction time during initiation and inhibition of speech and hand movement. Hum. Mov. Sci. 54, 41–50. https://doi.org/10.1016/j.humov.2017.03.005.

Kéri, S., Benedek, G., 2009. Visual pathway deficit in female fragile X premutation carriers: a potential endophenotype. Brain Cogn. 69 (2), 291–295. https://doi.org/10.1016/j.bandc.2008.08.002.

Kéri, S., Benedek, G., 2012. Why is vision impaired in fragile X premutation carriers? The role of fragile X mental retardation protein and potential FMR1 mRNA toxicity. Neuroscience 206, 183–189. https://doi.org/10.1016/j.neuroscience.2012.01.005.

Kim, S.Y., Tassone, F., Simon, T.J., Rivera, S.M., 2014. Altered neural activity in the 'when' pathway during temporal processing in fragile X premutation carriers. Behav. Brain Res. 261, 240–248. https://doi.org/10.1016/j.bbr.2013.12.044.

Kraan, C.M., Hocking, D.R., Georgiou-Karistianis, N., Metcalfe, S.A., Archibald, A.D., Fielding, J., et al., 2014. Age and CGG-repeat length are associated with neuromotor impairments in at-risk females with the FMR1 premutation. Neurobiol. Aging 35(9), 2179 e2177–2113. doi: 10.1016/j.neurobiolaging.2014.03.018.

Laidlaw, D.H., Bilodeau, M., Enoka, R.M., 2000. Steadiness is reduced and motor unit discharge is more variable in old adults. Muscle Nerve 23 (4), 600–612. https://doi.org/10.1002/(SICI)1097-4598(200004)23:4<600::AID-MUS20>3.0.CO;2-D.

Leehey, M.A., Berry-Kravis, E., Goetz, C.G., Zhang, L., Hall, D.A., Li, L., et al., 2008. FMR1 CGG repeat length predicts motor dysfunction in premutation carriers. Neurology 70 (16 Pt 2), 1397–1402. https://doi.org/10.1212/01.wnl.0000281692.98200.f5.

Loesch, D.Z., Bui, M.Q., Hammersley, E., Schneider, A., Storey, E., Stimpson, P., et al., 2015. Psychological status in female carriers of premutation FMR1 allele showing a complex relationship with the size of CGG expansion. Clin. Genet. 87 (2), 173–178. https://doi.org/10.1111/cge.12347.

Lüdecke, D., 2019. sjstats: Statistical Functions for Regression Models (Version 0.17.7).

Macaluso, E., Frith, C.D., Driver, J., 2002. Crossmodal spatial influences of touch on

extrastriate visual areas take current gaze direction into account. Neuron 34 (4), 647–658. https://doi.org/10.1016/S0896-6273(02)00678-5.

McKinney, W.S., Wang, Z., Kelly, S., Khemani, P., Lui, S., White, S.P., et al., 2019. Precision sensorimotor control in aging FMR1 gene premutation carriers. Front. Integr. Neurosci. 13, 56. https://doi.org/10.3389/fnint.2019.00056.

McLaren, D.G., Ries, M.L., Xu, G., Johnson, S.C., 2012. A generalized form of context-dependent psychophysiological interactions (gPPI): a comparison to standard approaches. Neuroimage 61 (4), 1277–1286. https://doi.org/10.1016/j.neuroimage.2012.03.068.

Neely, K.A., Coombes, S.A., Planetta, P.J., Vaillancourt, D.E., 2013. Segregated and overlapping neural circuits exist for the production of static and dynamic precision grip force. Hum. Brain Mapp. 34 (3), 698–712. https://doi.org/10.1002/hbm.21467.

Niu, Y.Q., Yang, J.C., Hall, D.A., Leehey, M.A., Tassone, F., Olichney, J.M., et al., 2014. Parkinsonism in fragile X-associated tremor/ataxia syndrome (FXTAS): revisited. Parkinsonism Relat. Disord. 20 (4), 456–459. https://doi.org/10.1016/j.parkreldis.2014.01.006.

O'Keefe, J.A., Robertson-Dick, E., Dunn, E.J., Li, Y., Deng, Y., Fiutko, A.N., et al., 2015. Characterization and early detection of balance deficits in fragile X premutation carriers with and without fragile X-associated tremor/ataxia syndrome (FXTAS). Cerebellum 14 (6), 650–662. https://doi.org/10.1007/s12311-015-0659-7.

O'Keefe, J.A., Robertson-Dick, E.E., Hall, D.A., Berry-Kravis, E., 2016. Gait and functional mobility deficits in fragile x-associated tremor/ataxia syndrome. Cerebellum 15 (4), 475–482. https://doi.org/10.1007/s12311-015-0714-4.

O'Keeffe, C., Taboada, L.P., Feerick, N., Gallagher, L., Lynch, T., Reilly, R.B., 2019. Complexity based measures of postural stability provide novel evidence of functional decline in fragile X premutation carriers. J. NeuroEng. Rehabil. 16 (1), 87. https://doi.org/10.1186/s12984-019-0560-6.

Park, S.H., Wang, Z., McKinney, W., Khemani, P., Lui, S., Christou, E.A., et al., 2019. Functional motor control deficits in older FMR1 premutation carriers. Exp. Brain Res. 237 (9), 2269–2278. https://doi.org/10.1007/s00221-019-05566-3.

Paulsen, J.S., Zimbelman, J.L., Hinton, S.C., Langbehn, D.R., Leveroni, C.L., Benjamin, M.L., et al., 2004. fMRI biomarker of early neuronal dysfunction in presymptomatic Huntington's Disease. AJNR Am. J. Neuroradiol. 25 (10), 1715–1721.

Prodoehl, J., Corcos, D.M., Vaillancourt, D.E., 2009. Basal ganglia mechanisms underlying precision grip force control. Neurosci. Biobehav. Rev. 33 (6), 900–908. https://doi.org/10.1016/j.neubiorev.2009.03.004.

Rathbun, D.L., Usrey, W.M., 2009. Geniculo-Striate Pathway. In: Binder, M.D., Hirokawa, N., Windhorst, U. (Eds.), Encyclopedia of Neuroscience. Springer Berlin Heidelberg, Berlin, Heidelberg, pp. 1707–1710.

Reilly, J.L., Lencer, R., Bishop, J.R., Keedy, S., Sweeney, J.A., 2008. Pharmacological treatment effects on eye movement control. Brain Cogn. 68 (3), 415–435. https://doi.org/10.1016/j.bandc.2008.08.026.

Remy, F., Mirrashed, F., Campbell, B., Richter, W., 2005. Verbal episodic memory impairment in Alzheimer's disease: a combined structural and functional MRI study. Neuroimage 25 (1), 253–266. https://doi.org/10.1016/j.neuroimage.2004.10.045.

Rodriguez-Revenga, L., Madrigal, I., Pagonabarraga, J., Xuncla, M., Badenas, C., Kulisevsky, J., et al., 2009. Penetrance of FMR1 premutation associated pathologies in fragile X syndrome families. Eur. J. Hum. Genet. 17 (10), 1359–1362. https://doi.org/10.1038/ejhg.2009.51.

Roid, G.H., 2003. Stanford-Binet Intelligence Scales, Fifth Edition: Technical Manual. Riverside Publishing, Itasca, IL.

Rowe, J.B., Hughes, L.E., Barker, R.A., Owen, A.M., 2010. Dynamic causal modelling of effective connectivity from fMRI: are results reproducible and sensitive to Parkinson's disease and its treatment? Neuroimage 52 (3), 1015–1026. https://doi.org/10.1016/j.neuroimage.2009.12.080.

Schmitz-Hubsch, T., Tezenas du Montcel, S., Baliko, L., Boesch, S., Bonato, S., Fancellu, R., et al., 2006. Reliability and validity of the International Cooperative Ataxia Rating Scale: a study in 156 spinocerebellar ataxia patients. Mov. Disord. 21 (5), 699–704. https://doi.org/10.1002/mds.20781.

Schoch, B., Regel, J.P., Frings, M., Gerwig, M., Maschke, M., Neuhauser, M., et al., 2007. Reliability and validity of ICARS in focal cerebellar lesions. Mov. Disord. 22 (15), 2162–2169. https://doi.org/10.1002/mds.21543.

Sellier, C., Buijsen, R.A.M., He, F., Natla, S., Jung, L., Tropel, P., et al., 2017. Translation of expanded CGG repeats into FMRpolyG is pathogenic and may contribute to fragile x tremor ataxia syndrome. Neuron 93 (2), 331–347. https://doi.org/10.1016/j.neuron.2016.12.016.

Shelton, A.L., Wang, J.Y., Fourie, E., Tassone, F., Chen, A., Frizzi, L., et al., 2018. Middle cerebellar peduncle width-a novel MRI biomarker for FXTAS? Front. Neurosci. 12, 379. https://doi.org/10.3389/fnins.2018.00379.

Sommer, U., Hummel, T., Cormann, K., Mueller, A., Frasnelli, J., Kropp, J., et al., 2004. Detection of presymptomatic Parkinson's disease: combining smell tests, transcranial sonography, and SPECT. Mov. Disord. 19 (10), 1196–1202. https://doi.org/10.1002/mds.20141.

Soontarapornchai, K., Maselli, R., Fenton-Farrell, G., Tassone, F., Hagerman, P.J., Hessl, D., et al., 2008. Abnormal nerve conduction features in fragile X premutation carriers. Arch. Neurol. 65 (4), 495–498. https://doi.org/10.1001/archneur.65.4.495.

Spraker, M.B., Corcos, D.M., Vaillancourt, D.E., 2009. Cortical and subcortical mechanisms for precisely controlled force generation and force relaxation. Cereb. Cortex 19 (11), 2640–2650. https://doi.org/10.1093/cercor/bhp015.

Stein, J.F., 1986. Role of the cerebellum in the visual guidance of movement. Nature 323 (6085), 217–221. https://doi.org/10.1038/323217a0.

Stein, J.F., Glickstein, M., 1992. Role of the cerebellum in visual guidance of movement. Physiol. Rev. 72 (4), 967–1017. https://doi.org/10.1152/physrev.1992.72.4.967.

Steyaert, J., Borghgraef, M., Fryns, J.P., 1994. Apparently enhanced visual information processing in female fragile X carriers: preliminary findings. Am. J. Med. Genet. 51 (4), 374–377. https://doi.org/10.1002/ajmg.1320510415.

Todd, P.K., Oh, S.Y., Krans, A., He, F., Sellier, C., Frazer, M., et al., 2013. CGG repeat-associated translation mediates neurodegeneration in fragile X tremor ataxia syndrome. Neuron 78 (3), 440–455. https://doi.org/10.1016/j.neuron.2013.03.026.

Trouillas, P., Takayanagi, T., Hallett, M., Currier, R.D., Subramony, S.H., Wessel, K., et al., 1997. International Cooperative Ataxia Rating Scale for pharmacological assessment of the cerebellar syndrome. The Ataxia Neuropharmacology Committee of the World Federation of Neurology. J. Neurol. Sci. 145 (2), 205–211. https://doi.org/10.1016/S0022-510X(96)00231-6.

Trujillo, J.P., Gerrits, N.J., Veltman, D.J., Berendse, H.W., van der Werf, Y.D., van den Heuvel, O.A., 2015. Reduced neural connectivity but increased task-related activity during working memory in de novo Parkinson patients. Hum. Brain Mapp. 36 (4), 1554–1566. https://doi.org/10.1002/hbm.22723.

Unschuld, P.G., Joel, S.E., Liu, X., Shanahan, M., Margolis, R.L., Biglan, K.M., et al., 2012. Impaired cortico-striatal functional connectivity in prodromal Huntington's Disease. Neurosci. Lett. 514 (2), 204–209. https://doi.org/10.1016/j.neulet.2012.02.095.

Vaillancourt, D.E., Larsson, L., Newell, K.M., 2003a. Effects of aging on force variability, single motor unit discharge patterns, and the structure of 10, 20, and 40 Hz EMG activity. Neurobiol. Aging 24 (1), 25–35. https://doi.org/10.1016/S0197-4580(02)00014-3.

Vaillancourt, D.E., Mayka, M.A., Corcos, D.M., 2006. Intermittent visuomotor processing in the human cerebellum, parietal cortex, and premotor cortex. J. Neurophysiol. 95 (2), 922–931. https://doi.org/10.1152/jn.00718.2005.

Vaillancourt, D.E., Newell, K.M., 2003. Aging and the time and frequency structure of force output variability. J. Appl. Physiol. (1985) 94 (3), 903–912. https://doi.org/10.1152/japplphysiol.00166.2002.

Vaillancourt, D.E., Thulborn, K.R., Corcos, D.M., 2003b. Neural basis for the processes that underlie visually guided and internally guided force control in humans. J. Neurophysiol. 90 (5), 3330–3340. https://doi.org/10.1152/jn.00394.2003.

Vittal, P., Pandya, S., Sharp, K., Berry-Kravis, E., Zhou, L., Ouyang, B., et al., 2018. ASFMR1 splice variant: a predictor of fragile X-associated tremor/ataxia syndrome. Neurol Genet 4 (4), e246. https://doi.org/10.1212/NXG.0000000000000246.

Wang, J.Y., Hessl, D., Hagerman, R.J., Simon, T.J., Tassone, F., Ferrer, E., et al., 2017. Abnormal trajectories in cerebellum and brainstem volumes in carriers of the fragile X premutation. Neurobiol. Aging 55, 11–19. https://doi.org/10.1016/j.neurobiolaging.2017.03.018.

Wang, J.Y., Hessl, D., Schneider, A., Tassone, F., Hagerman, R.J., Rivera, S.M., 2013. Fragile X-associated tremor/ataxia syndrome: influence of the FMR1 gene on motor fiber tracts in males with normal and premutation alleles. JAMA Neurol. 70 (8), 1022–1029. https://doi.org/10.1001/jamaneurol.2013.2934.

Wang, J.Y., Hessl, D.H., Hagerman, R.J., Tassone, F., Rivera, S.M., 2012. Age-dependent structural connectivity effects in fragile x premutation. Arch. Neurol. 69 (4), 482–489. https://doi.org/10.1001/archneurol.2011.2023.

Wang, Z., Khemani, P., Schmitt, L.M., Lui, S., Mosconi, M.W., 2019. Static and dynamic postural control deficits in aging fragile X mental retardation 1 (FMR1) gene premutation carriers. J. Neurodev. Disord. 11 (1), 2. https://doi.org/10.1186/s11689-018-9261-x.

Wang, Z., Magnon, G.C., White, S.P., Greene, R.K., Vaillancourt, D.E., Mosconi, M.W., 2015. Individuals with autism spectrum disorder show abnormalities during initial and subsequent phases of precision gripping. J. Neurophysiol. 113 (7), 1989–2001. https://doi.org/10.1152/jn.00661.2014.

Wolpert, D.M., Miall, R.C., Kawato, M., 1998. Internal models in the cerebellum. Trends Cogn. Sci. 2 (9), 338–347. https://doi.org/10.1016/S1364-6613(98)01221-2.